CrossMark

ORIGINAL ARTICLE

Permeability distribution in the Lahendong geothermal field: A blind fault captured by thermal–hydraulic simulation

Maren Brehme[1] · Guido Blöcher[1] · Mauro Cacace[1] · Yustin Kamah[2] · Martin Sauter[3] · Günter Zimmermann[1]

Abstract Subsurface fluid flow of reservoirs in active tectonic regions is mainly controlled by permeability of fault zones. Therefore, the characterization of fault zones is an important step toward performance assessment of a reservoir. The fluid flow is controlled also by pressure and temperature conditions. In this context, we simulated pressure and temperature fields to elaborate on the influence of permeability on subsurface fluid flow in the Lahendong geothermal reservoir. Thermal–hydraulic simulation is performed using a finite element approach. Adjusting the permeability through 370 different cases, modeling results converged to the observed data within a misfit range of 0–7 %. The best fitting models identified a deep-seated fault that has previously not been traced at the surface. Simulated temperature distribution suggests a prominent convective heat flow, driven by an upward migrating and SW–NE oriented fluid flow. This hydraulic gradient causes a pressure drop along the reservoir. High-pressure patterns are used to constrain recharge areas, in addition to infiltration measurements. Discharge flow occurs from SW to NE migrating also upward toward the hot springs. In that frame, thermal–hydraulic simulations identified previously unresolved subsurface faults, which now allow a better understanding of the subsurface permeability and its influence on fluid flow.

Introduction

Geothermal energy is an essential component to supply future energy demands. It requires developing new geothermal sites and improving the performance of existing systems to satisfy continuously growing demand. The productivity of a geothermal field mainly depends on subsurface fluid flow, which in active tectonic regions is controlled by permeability of fault zones (Moeck 2014). In that frame, the primary focus is on locating and characterizing faulted areas in geothermal fields. This study employs numerical modeling to allocate and quantify permeability anisotropies and discontinuities, e.g., faults, in order to understand their influence on subsurface fluid flow in geothermal reservoirs.

Numerical models have been increasingly used to understand the setup and productivity of geothermal systems. A general overview of geothermal models has been given by O'Sullivan et al. (2001). Additionally, there are several sites exemplifying similar characteristics as in Lahendong. The underground movement of hot and cold fluids has been modeled for geothermal fields in New Zealand (Kaya et al. 2014). The Kakkonda geothermal site, e.g., consists of two reservoirs at various depths with different fluid properties. There, results from fluid flow analysis show the importance of fractures for fluid transport enhancing the recharge or discharge in the reservoir

✉ Maren Brehme
brehme@gfz-potsdam.de

1 Helmholtz Centre Potsdam – GFZ German Research Centre for Geosciences, Telegrafenberg, 14473 Potsdam, Germany

2 Upstream Technology Center Pertamina, Jl. Medan Merdeka Timur no. 6, Jakarta, Indonesia

3 Applied Geology, University of Göttingen, Goldschmidtstraße. 3, 37077 Göttingen, Germany

(McGuinness et al. 1995). Generally, faults acting as preferential fluid path ways significantly change the pressure and temperature field in the reservoir (Cherubini et al. 2013). Models for the Seferihisar–Balçova field focus on the fluid flow inside of faults. Results show an enhanced upward heat transport through fluids from bottom of the geothermal system (Magri et al. 2011).

Our test ground is the Lahendong geothermal field located in Sulawesi, Indonesia. The field is owned and operated by P.T. Pertamina Geothermal Energy and hosts a power plant with a production capacity of 80 MWe. There, geothermal exploration started in the early 1970s including geophysical and geohydrochemical approaches. It is a water-dominated magmatic structurally controlled system. Faults generally act as across-fault fluid barriers and along-fault fluid conductors (Brehme et al. 2014). As a result, hot springs mainly appear on the top of vertically permeable faults at the surface. Available numerous drilling and surface measurements allowed a detailed characterization of the geological and hydrogeological setting of the area (Fig. 1; Brehme et al. 2011, 2013, 2014, 2016; Wiegand et al. 2013). The model presented here is developed for investigating subsurface fluid flow and the permeability distribution including the fault zones in the Lahendong geothermal field. Below, the geological structure of the field is presented followed by an introduction to the modeling approach.

Detailed investigation of subsurface permeability distribution is a crucial step for site selection and smart drilling strategies. The numerical simulations presented will provide insight into understanding the subsurface fluid flow considering the hydraulic conductivity of faults. It ensures productive as well as sustainable operation of geothermal fields avoiding risks, such as drilling into non-fractured or cold zones, and targeting highly corroding waters. Although the target area is Lahendong, the general workflow is applicable for other geothermal sites consisting of similar constraints.

Reservoir characterization

Hydrogeology

The overall driving force for the fluid flow is the SW–NE oriented natural hydraulic gradient in the Lahendong geothermal system. The direction of fluid flow varies through the geothermal site due to horizontal partitioning of the reservoir by relatively less permeable fault zones (Brehme et al. 2014). The basic sections are located in the
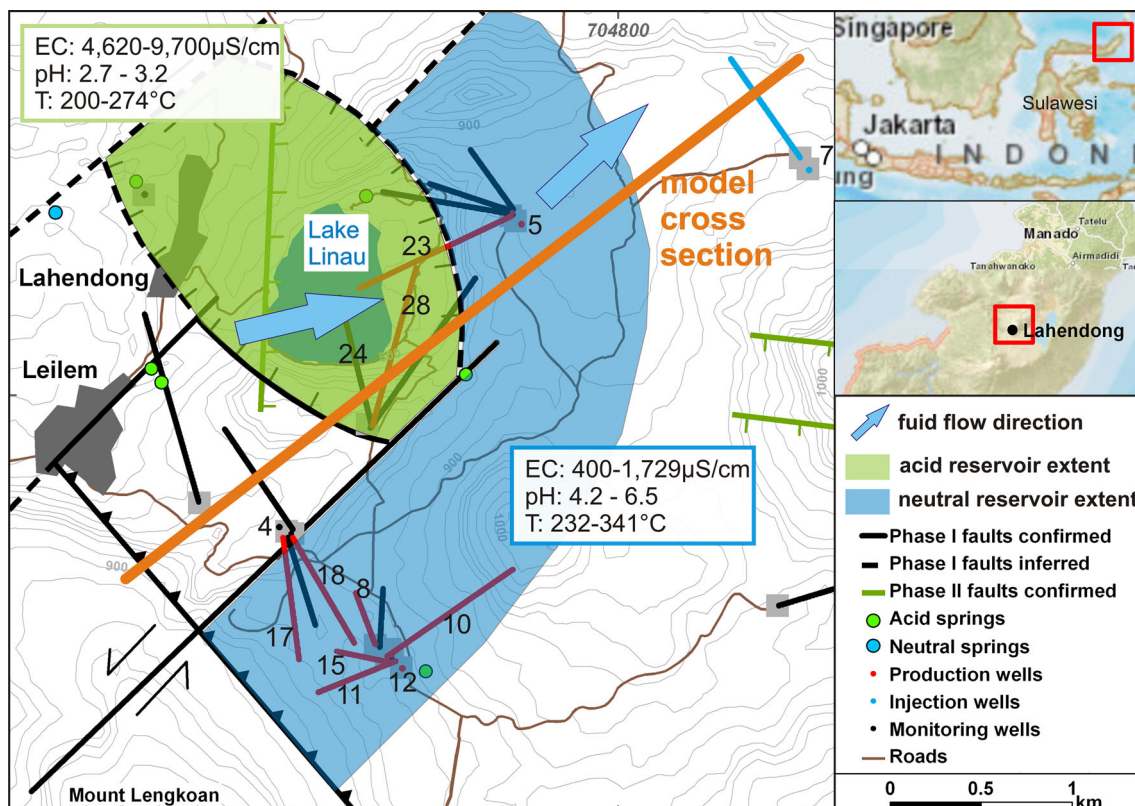

Fig. 1 Topographic map of the study area with geological features, water and rock sample locations, and model cross section

south, in the east, and beneath Lake Linau. Beneath Lake Linau, the direction of fluid flow is slightly rotated to WSW–ENE (Fig. 1). Also, types of fluid change from one section to another, e.g., an acidic highly saline-type beneath Lake Linau and a neutral low saline-type south and east of Lake Linau (Fig. 1). The impermeable structure across faults prevent the fluids from diluting each other (Brehme et al. 2016). However, faults are rather permeable along the vertical axis, which allows recharge of the system through the faults. Rainwater infiltrates at a fault in the SW, at Mt. Lengkoan, and creek water infiltrates into the normal faults at Lake Linau (Fig. 2). The hydrothermal system discharges into Lake Linau and toward the NE, as driven by the hydraulic gradient (Brehme et al. 2014).

The fracture network along the area is characterized by strike slip faults and normal faults. The sinistral faults strike N 40° and steeply dip toward the SE. Left step over on the strike slip faults forms an extension basin in the central study area. Normal faults at the extension basin strike NW and dip 70°–80° beneath Lake Linau (Brehme et al. 2014).

Lithology

Lahendong area is mainly characterized by Pre-, Post- and Tondano formation of Plio- to Pleistocene age (Koestono et al. 2010). The rocks are typically andesite, volcanic breccia, and tuff. Those types have been sampled from borehole cores and used to determine porosity, permeability, and thermal conductivity. Effective porosity and matrix permeability have been analyzed using a cylindrical-shaped specimen with a dimension of 5 cm x 5 cm × 2.5 cm oriented parallel to the coring (Brehme et al. 2016). Thermal conductivity has been measured on plain sections of dried cores. The experimental setup consists of a gas permeameter for determining matrix permeability (Milsch et al. 2011), of an helium pycnometry for effective porosity measurements (Johnson-Maynard et al. 1994) and of an optical scanner for thermal conductivity measurements (Popov et al. 1999). These parameters have been measured and averaged for the three rock types (Brehme et al. 2016; Table 1). Andesite has an effective porosity of 3.7 %, a permeability of 2.1×10^{-14} m^2, and a thermal conductivity of 1.8 W m^{-1} K^{-1} (dry) or 2.2 W m^{-1} K^{-1} (saturated). Tuff has a porosity of 7.7 % but the lowest permeability of 2.0×10^{-15} m^2 and a thermal conductivity of 1.6 W m^{-1} K^{-1} (dry) or 2.1 W m^{-1} K^{-1} (saturated). Volcanic breccia is a permeable layer with an effective porosity of 10.5 %, a permeability of 2.3×10^{-14} m^2, and a thermal conductivity of 1.6 W m^{-1} K^{-1} (dry) or 2.5 W m^{-1} K^{-1} (saturated). Reservoir rocks reflect generally low matrix permeability suggesting fracture-controlled fluid flow throughout the aquifer (Brehme et al. 2016).

Model setup

Model geometry

Numerical models developed for the study area represent the initial conditions of the reservoir before production or injection start. For simulation, the commercial finite
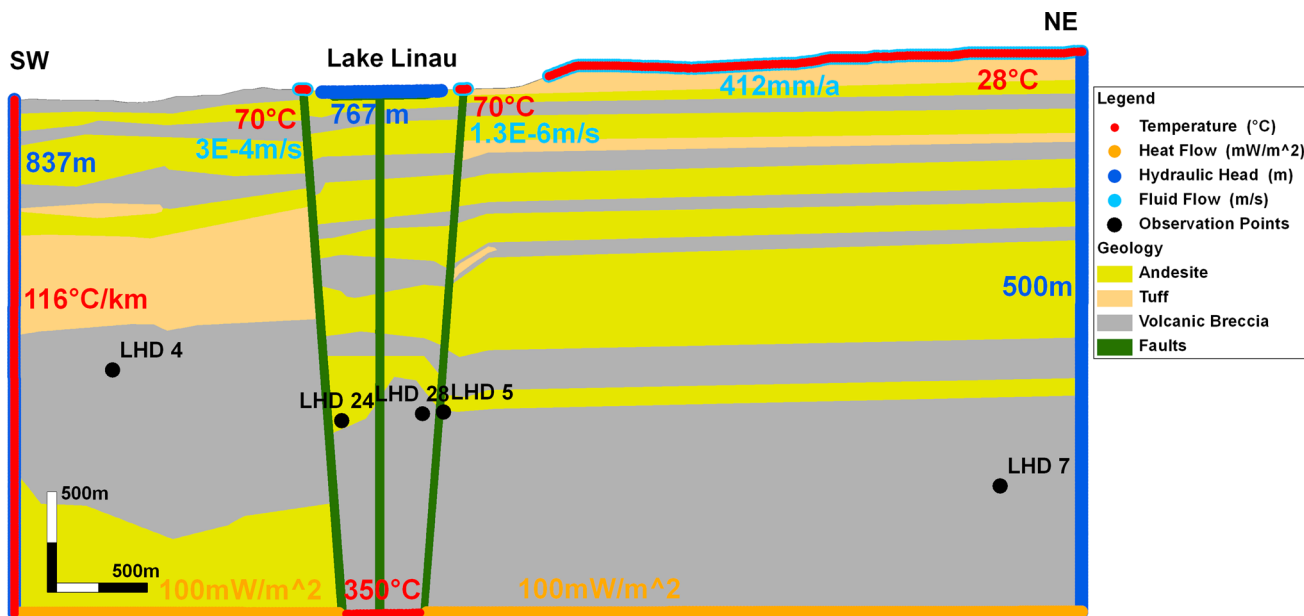

Fig. 2 Cross section of the modeled area with geological structure, boundary conditions, and location of observation points

Table 1 Thermal and hydraulic parameters of the Lahendong reservoir rocks measured in laboratory (Brehme et al. 2016)

Sample (name, depth)	Rock type	Effective porosity (%)	Thermal conductivity dry (W m^{-1} K^{-1})	Thermal conductivity saturated (W m^{-1} K^{-1})	Matrix permeability (m^2)
LHD1 500–501	A	1.1	(LHD1 550) 2.0	(LHD1 550) 2.2	
LHD1 801–802	B	14.5	1.6	2.4	1.5×10^{-14}
LHD1 1000–1001	T	5.0	1.8	2.2	8.9×10^{-16}
LHD1 2100–2101	T	7.2	1.4	2.0	3.3×10^{-15}
LHD2 300–302	A	12.5			6.1×10^{-14}
LHD3 2201–2203	B	5.7	2.1	2.4	1.5×10^{-14}
LHD4 652–653	B	6.3			1.3×10^{-14}
LHD4 850–852	A	1.6	1.8	2.0	2.3×10^{-14}
LHD4 1001–1002	B	16.4	1.4	2.7	6.8×10^{-14}
LHD4 2304–2305	A	1.6	1.8	2.7	3.4×10^{-16}
LHD5 602–603	B	16.3	1.4	2.3	1.1×10^{-14}
LHD5 752–753	A	2.7			1.1×10^{-16}
LHD5 1102–1103	A	5.2			7.9×10^{-14}
LHD5 1404–1406	A	3.6	1.9	2.3	3.0×10^{-15}
LHD5 1575–1576	A	0.6			7.9×10^{-18}
LHD7 901–902,3	A	4.6	1.5	1.7	7.2×10^{-16}
LHD7 1567.8–1568	T	11.0	1.6	2.2	1.7×10^{-15}
LHD7 1756–1758	B	3.9	2.1	2.7	1.7×10^{-14}
Average values	Andesite (A)	3.7	1.8	2.2	2.1×10^{-14}
	Breccia (B)	10.5	1.6	2.5	2.3×10^{-14}
	Tuff (T)	7.7	1.6	2.1	2.0×10^{-15}

element software FEFLOW is used to model pressure-driven and thermally induced fluid flow including viscosity changes. Governing equations for fluid flow and heat transport in saturated porous media are derived from conservation principles of linear momentum, mass, and energy (DHI-Wasy 2009). Details on the software and the parameterization can be found in Diersch (2014).

The model geometry is a 2D vertical SW–NE trending cross section extending 6 km in horizontal and 3 km in vertical direction. The direction of the profile has been selected to cover all relevant processes in the Lahendong geothermal field: It cuts major faults and the production and injection wells, which are used for temperature and pressure calibration. Furthermore, it is parallel to the groundwater flow direction, showing major fluid flow activities. The homogeneous and isotropic geological layers in the model are stratified nearly horizontally. Faults in the middle of the model, striking perpendicular to the cross section, dip with 84° toward a cooling pluton beneath Lake Linau. Details on structural and geological components of the modeled region have been presented in Brehme et al. (2014).

The mesh used for the numerical simulation in FEFLOW consists of 45,264 nodes and 89,320 elements that are denser surrounding the faults because of expected gradients due to parameter contrasts. Material properties of

elements are permeability, porosity, and thermal conductivity and set according to laboratory measurements (Table 1). However, properties of the faults and Lake Linau are slightly adapted to specific conditions. The definitions for the modeled grids along the faults are as follows: porosity is 30 % and thermal conductivity is 1.8 W m^{-1} K^{-1}. Corresponding grids for Lake Linau are defined by a porosity of 100 % and a thermal conductivity of 0.6 W m^{-1} K^{-1}. The model simulates fluid flow and thermal transport in saturated media in steady state.

Initial values and boundary conditions

Fluid flow boundary conditions in the model describe groundwater heads and recharge amounts (Table 2; Fig. 2). The hydraulic head at the SW model boundary is 837 m and 500 m at the NE boundary. The SW hydraulic head represents infiltration of surface water into a fault, striking perpendicular to the model. Hydraulic head at the NE border is adapted to borehole measurements in that area (Brehme et al. 2014). Infiltration into the fault zones at Lake Linau is described by fluid flux boundary conditions. The quantity is 3.0×10^{-4} m s^{-1} for the SW and 1.3×10^{-6} m s^{-1} at the NE fault distributed over 40 m fault width. Groundwater recharge is set to 412 mm a^{-1} at the NE top surface (Table 2; Fig. 2). Fluid movement in

Table 2 Boundary condition specifications and respective references of database

Type of Boundary condition	SW model boundary	SW fault	Lake	Cooling pluton	NE fault	NE model surface	NE model boundary	Bottom of model
Fluid flow								
Hydraulic head (m)	837 bore log measurement[a]		767 surface elevation[a]				500 bore log measurement[a]	
Fluid flux (m s^{-1})		3.0 x 10^{-4} field measurement[a]			1.3 x 10^{-4} field measurement[a]	1.3 x 10^{8} calculation[b]		
Heat transport								
Temperature (°C)	116 °C km^{-1} bore log measurement[a]	70 estimation[a]		350 bore log measurement[a]	70 estimation[a]	28 field measurement[a]		
Heat flux (mW m^{-2})								100[c]
Material properties	See Table 1							

[a] Brehme et al. (2014)

[b] DWD (2007), Hölting and Coldewey (2005), Saghravani et al. (2013)

[c] Delisle et al. (1998), Nagao and Uyeda (1995), Neben et al. (1998)

the model domain is constrained by no-flow boundary at the bottom, recharge through the surrounding fault zones, and the low hydraulic heads in the NE model area. Discharge of the system in the central study area is mainly toward Lake Linau and across the NE model boundary. Initial hydraulic head for the whole model domain is 500 m.

The heat transport boundary conditions are time-invariant, fixed temperatures, and heat flux (Table 2; Fig. 2). Thermal gradient is 116 °C km^{-1} at the SW model boundary, and the temperature is constant 350 °C at the pluton. Temperature of water infiltrating into faults and here mixing with shallow warm groundwater is 70 °C, while surface groundwater recharge is at 28 °C. Temperature values are obtained from field and bore log measurements (Brehme et al. 2014). Heat flux is set to 100 mW m^{-2} at the bottom model boundary (Table 2; Fig. 2). This value is fixed based on the studies from Delisle et al. (1998), Nagao and Uyeda (1995), and Neben et al. (1998). Initial temperature for the model domain is set as 116 °C km^{-1}, according to the local thermal gradient.

Permeability determination

Initial values for permeability are defined based on laboratory measurements (Table 1). After each simulation run, modeled and measured temperature and pressure values have been compared at indicated observation points. In case of poor matching (errors >10 %), permeability has been adjusted until satisfactory results have been achieved. Beneath lake Linau, simulation results showed locally strong discrepancies between modeled and measured pressure and temperature (errors >45 %). Adjustment of permeability in geological layers, infiltration rates into faults, or hydraulic heads did not lead to acceptable results. Only the implementation of strong permeability anisotropy throughout whole depth, i.e., an additional fault, resulted in minimization of errors (0–7 %). Implementation has been accomplished by mesh adaptation to ensure appropriate behavior around the fault. By this procedure, permeability anisotropies have been located and characterized in detail throughout the model.

In general, defining a direction-dependent permeability improves the data fit rather than using similar permeabilities in all directions. This is probably due to the fractures increasing the permeability mostly in vertical direction.

Porosity and thermal conductivity remained constant throughout simulation. Variation in porosity is negligible because it would directly be reflected in permeability, while thermal conductivity differences would only affect conductive heat transport, which is not dominant in the Lahendong area (Ondrak et al. 1998; Brehme et al. 2014).

Results

Numerical simulation is performed to obtain the best fit to the measured data changing the absolute and relative permeability in geological elements. Relative permeability refers to different permeabilities in horizontal and vertical direction. As a main result, a blind fault has been recognized beneath Lake Linau, which has not been known from former studies. Simulated pressure and temperature are measured at five selected observation points, which represent boreholes with available bore logs for pressure and temperature. Details on data are given in Fig. 6. The model with best data fit, out of 370 different models, is considered to generate the final model developed for Lahendong.

Permeability distribution and identification of a blind fault

Distribution of permeability patterns in the reservoir has been conceived comparing temperature and pressure data in several wells. Especially beneath Lake Linau, closely located wells show high variations in temperature and pressure. A drop of 100 °C and 18 bar along 300 m distance has been observed between well LHD 24 and LHD 28. Models first showed high discrepancies between modeled and measured values in this area. However, after implementing another high anisotropic permeable structure between the observation points, models resulted in satisfactory results. The structure has ten times higher vertical

permeability than horizontal permeability. This structure is assumed to be another fault zone located between two known faults with vertical dip and NW strike. This fault shows no trace at surface, because it is covered by Lake Linau.

Generally, modeled permeability distribution in the Lahendong reservoir is direction-dependent and overprints the lithology. Modeled permeability is generally higher than measured ones in the order of up to four magnitudes. This is due to fracture patterns, which are not detectable at core-sample scale. Permeability patterns directly affect subsurface fluid flow and temperature and pressure distribution.

Permeability in the faulted zones and surroundings is lowest in the study area. Especially the middle and NE fault, the shallow area beneath SW Lake Linau and the deep NE section of the NE fault show low permeabilities between 10^{-13} and 10^{-14} m^2 (Fig. 3). The area between the middle and NE fault, the deep section NE of the SW fault, the SW fault itself and the whole model area toward the SW and NE boundary show higher permeabilities of 10^{-10} and 10^{-12} m^2 (Fig. 3).

Permeability varies not only within the modeled area, but also in vertical and horizontal direction. In faults and the deep reservoir section in the NE, permeability is by a factor of 10 higher in the vertical direction than in the horizontal direction (Fig. 3). In the areas between faults, permeability is in some parts by a factor of 10–100 lower in the vertical direction. In the rest of the model, vertical and horizontal permeability do not differ (Fig. 3).
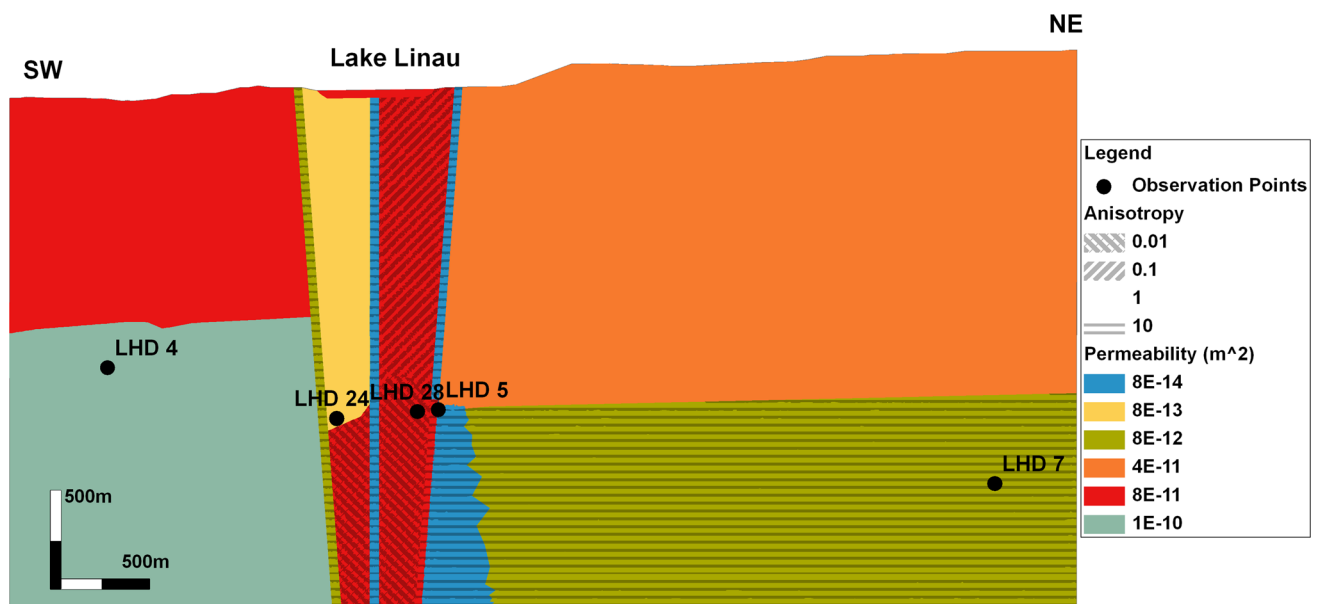

Fig. 3 Final adapted permeability and anisotropy distribution throughout the model domain. Anisotropy shows the relation between vertical and horizontal permeability, if anisotropy >1 vertical permeability is higher than horizontal permeability
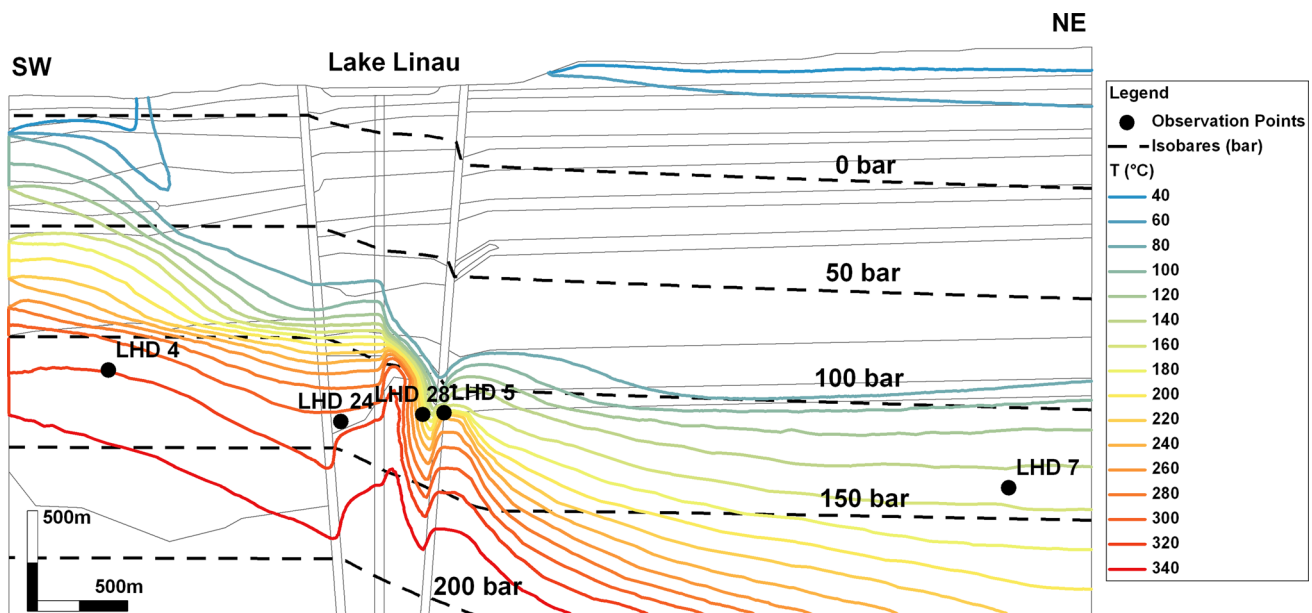
Fig. 4 Modeled temperature and pressure distribution in the study area shows high-pressure fields in the SW and convective heat transport with rising hot fluids and infiltration of cooler water through faults

Pressure distribution

The pressure distribution in the study area is controlled by groundwater flow in low permeable rocks and vertically high permeable fault zones. Isobars drop following the natural hydraulic gradient from SW to NE. The SW section of the system shows higher pressures, which is caused by infiltration from higher elevations in the SW. Some wells existing in this region are of artesian-type. Overpressure releases through high permeable zones beneath Lake Linau and discharges toward surface. The pressure drop is up to 20 bars across the faults (Fig. 4).

Temperature distribution

Temperature distribution along the Lahendong geothermal reservoir suggests that convective heat transport is the dominating process in the reservoir rocks. Isotherms generally follow the SW–NE oriented flow pattern, the rise and the infiltration of fluids. Upwelling of isotherms between the faults verifies water rise toward Lake Linau. Infiltration of cold water causes down welling of isotherms particularly on the northeast section of the model. Temperature is locally increased at the bottom of the model surrounding the pluton (Fig. 4).

Subsurface fluid flow

The absolute and horizontal/vertical permeability distribution controls local fluid flow in the Lahendong reservoir.

The general fluid flow, driven by the natural pressure gradient, is oriented from SW to NE. Vertical infiltration occurs at faults at Lake Linau and at the SW boundary. Discharge is across the NE model boundary (Fig. 5). The more detailed flow patterns can be observed with streamlines, which show a fluid flow along highly permeable areas. Calculated streamlines describe particle flow within the model domain. A forward calculation shows how infiltrating water at the SW model boundary distributes through the reservoir. The backward calculation shows the source of fluid particles arriving at the NE model boundary (Fig. 5). Patterns show that hot groundwater flows toward the faults beneath Lake Linau, where the fluid flow is disturbed by a rise in temperature and vertically high permeable layers. This causes a rise of groundwater in this model area (red forward streamlines in Fig. 5). At the same time, cold water infiltrates into high permeable areas and distributes over the NE model domain (blue backward streamlines in Fig. 5). It is clearly seen that the composition of the NE reservoir domain is dominated by coldwater infiltration into faults, while the production areas are characterized by hot water flow (Fig. 5).

Discussion

Investigation of subsurface fluid flow in geothermal reservoirs is crucial for sustainable exploitation avoiding drilling into less productive areas. Subsurface fluid flow might be locally influenced by fault zones or physical
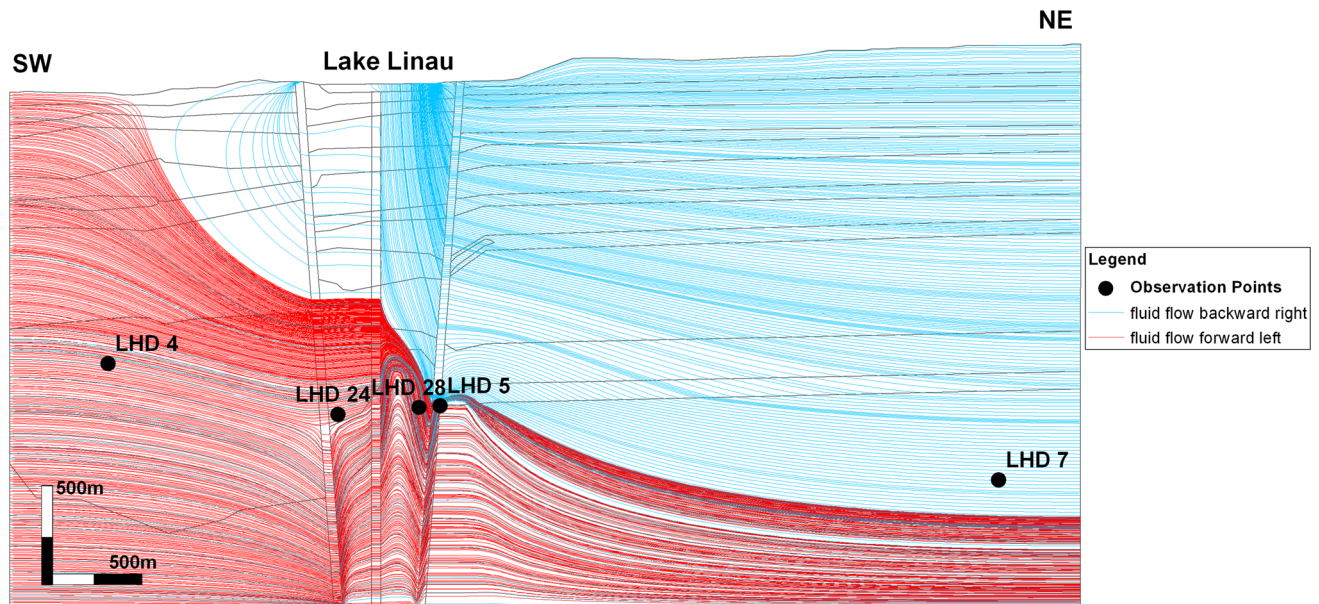
Fig. 5 Model domain with calculated streamlines, in *red*: forward streamlines follow hydraulic gradient from SW model boundary towards NE, in *blue*: backward streamlines representing infiltrating cold water flowing towards NE model boundary

properties of water (i.e. viscosity). The influence of these parameters on the fluid flow has been investigated in Lahendong geothermal reservoir using hydraulic–thermal simulations. Simulation results show the detailed permeability distribution in the reservoir including location of an additional fault zone.

Matching of measured and simulated temperature and pressure has been used as a tool for resolving the permeability distribution. Temperature and pressure have been iteratively determined at several observation points (Fig. 2). Generally, modeled values are in good agreement with observed ones (Fig. 6). Nevertheless, some observation points give slightly different values for both pressure and temperature (LHD 4 and LHD 7) or only temperature (LHD 24). This is probably due to the complicated flow processes or strong small-scale structural variation in fractured and faulted areas. Furthermore, density variations, which could have not been included into simulation due to high temperatures, could cause variation of fluid pressure. However, the average deviation of simulated pressure and temperature is 1 %.

Implemented model parameters are porosity, permeability, and heat conductivity. From those parameters, only permeability has been tested in a specific range during simulation. The influence of porosity and heat conductivity on fluid flow is negligible due to dominating convective heat flow (Ondrak et al. 1998). Values implemented in the model are based on measured permeabilities, which represent matrix permeability of rocks.

The measured matrix permeability, representing permeability in horizontal direction, is 1.5×10^{-14} m^2 on average, which remains within typical permeability range for fractured igneous rocks (Schön 2004). Permeability for volcanic breccias ranges typically between 3×10^{-15} and 5×10^{-12} m^2 and tuff permeabilities range between 7×10^{-17} and 7×10^{-12} m^2 (Klavetter and Peters 1987). In the Wairakei geothermal field, simulating the impermeable layers resulted in permeabilities of 10^{-18} and 10^{-14} m^2, in horizontal and vertical axis, respectively (Mercer and Faust 1979).

However, permeability in reservoir rocks might be locally increased due to fracture formation. It might also be decreased due to alteration and sealing in faults. In Lahendong, modeled permeability can be up to four magnitudes higher than measured ones in faulted areas. This is caused by fractures, which are not detectable in core scale. Moreover, in fault cores, it is by a factor of 10 higher in vertical direction than in horizontal direction. However, in areas between faults (fault gauge), permeability is in some parts by a factor of 10–100 lower in the vertical direction. Adaptation of permeability ensures a fit to measured temperature and pressure data.

Permeability in fractured areas is the main factor influencing subsurface fluid flow and temperature distribution in the Lahendong reservoir area. Subsurface fluid flow is driven by local hydraulic heads, which show high variations at different sections of the study area. Consequently, convective heat distribution leads to high temperature variation along the reservoir. These phenomena are observed in Lahendong as well as comparable fields. In New Mexico, water level drops of 30–100 m are observed across several fault zones (Haneberg 1995). High
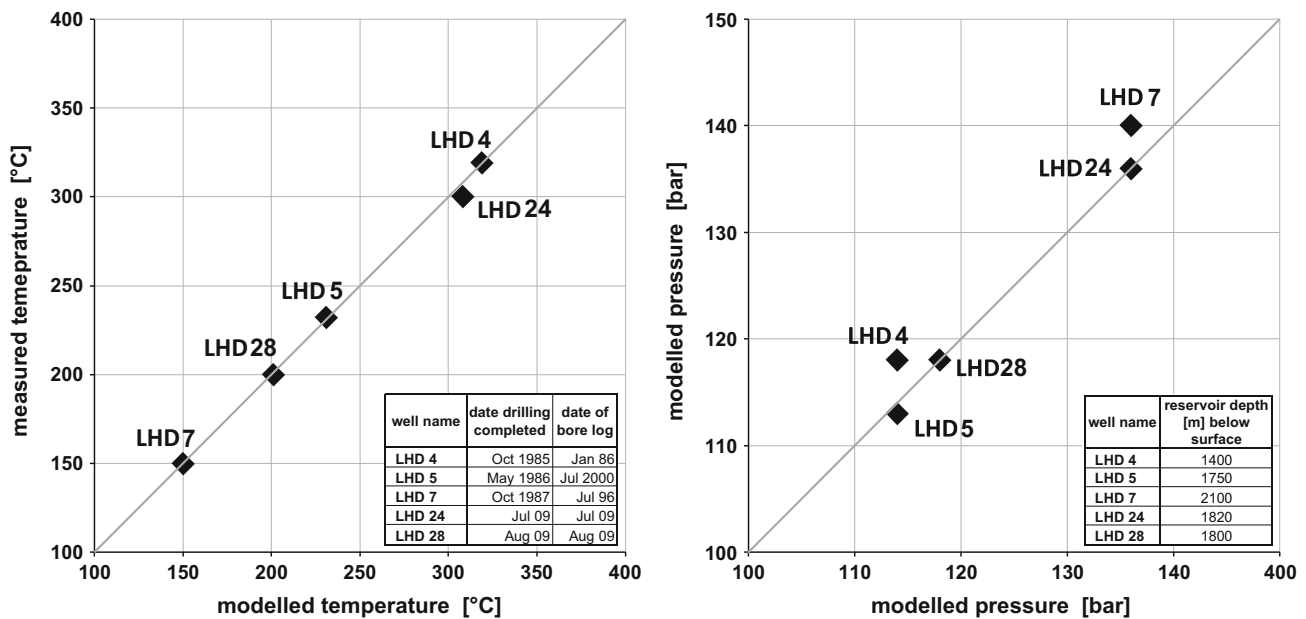
well name	date drilling completed	date of bore log
LHD 4	Oct 1985	Jan 86
LHD 5	May 1986	Jul 2000
LHD 7	Oct 1987	Jul 96
LHD 24	Jul 09	Jul 09
LHD 28	Aug 09	Aug 09

well name	reservoir depth [m] below surface
LHD 4	1400
LHD 5	1750
LHD 7	2100
LHD 24	1820
LHD 28	1800

Fig. 6 Modeled versus measured temperature and pressure at selected observation points. Well specifications and measured data from Brehme et al. (2014)

temperature drops and upwelling of isotherms indicate that fault zones control the fluid flow in the Lake Long and Valentine fields, USA (Hooper 1991). The analysis of fluid pressure differences at the Alpine fault, New Zealand, allowed to characterize the change in permeability between hanging and footwall blocks (Sutherland et al. 2012).

In summary, high pressure or temperature gradients are indicators for fluid barriers between observation points. In other words, reservoir sections of different properties are separated by horizontally less permeable faults. In Lahendong, most significant fluid barriers are faults to the SW and to the NE of Lake Linau. Across these barriers, the pressure drops up to 20 bars. A similar pattern has been measured in bore logs beneath Lake Linau, where no surface trace of a fault had been observed in former studies. However, only by implementing another fault, modeled and measured values could have been adapted. The recently identified fault zone beneath Lake Linau remains under lake water and therefore is only traceable by this kind of reservoir modeling.

Additionally to fault identification, the internal structure of known fault zones has been understood in detail. The NE fault, i.e., shows a displacement at 2 km depth. The detailed trend has been understood by permeability adaptation in this area.

Due to low permeability in horizontal direction in the faults, fluids propagate mostly vertically toward the hot springs at surface. It also allows surface water to infiltrate into the reservoir in case the pressure within the fault zone is low enough (Fig. 5). This vertical fluid movement

eventually controls the temperature distribution in the reservoir. Upward migration of deep hot water increases the temperature, while infiltration of cold surface water causes local drop of temperature.

In summary, the most important factors influencing the reliability of numerical reservoir models are absolute and different horizontal and vertical permeability. However, a permeability adaptation has been done for each geological layer; the vertical permeability anomalies are overprinting those layers and are constraining the regional groundwater flow. Those permeabilities of fractures directly influence the productivity of the reservoir (Cherubini et al. 2013). Therefore, their permeability characteristics should be investigated in detail.

In a previous study, a numerical model for the Lahendong site has been set up in TOUGH2 and aimed at forecasting the reservoir behavior during exploitation until the year 2036. With a production of 60 MWe, it predicts a pressure drop of 10 bars. However, the forecast results are uncertain due to lack of measured pressure draw down data (Yani 2006). Accordingly, the next steps of the presented study should include a realistic production and injection scenario in order to support sustainable reservoir exploitation. Furthermore, chemical characteristics could be considered to achieve reliable production setups, because hydrochemical processes play an important role in the Lahendong reservoir (Brehme et al. 2016). Presented models from this study provide important information on fluid flow in the water-dominated Lahendong reservoir. However, additional two-phase flow models of the

Lahendong area are in progress to understand the influence of steam driven fluid flow in this high-temperature system.

Conclusion

The primary focus of this study is to understand the influence of fault zones and permeability patterns on subsurface fluid flow in geothermal reservoirs. The fluid flow mainly depends on rock and fault zone permeability. These processes have been considered in numerical models, which simulate local temperature and pressure conditions.

The numerical models represent the initial reservoir conditions, which refers to the case before production starts. Models are developed based on the conceptual models of the study area, which explain reservoir geometry, geological structures, temperature, and hydraulic conditions. Temperature and pressure well-logs have been used for model calibration.

Vertical and horizontal fluid flow is mainly controlled by fault permeability. This characteristic is used to simulate different reservoir sections, and vertical fluid rise toward the surface. By stepwise adaptation of permeability fields, based on observed temperature and pressure gradients, an additional blind fault zone can be identified beneath Lake Linau. Temperature and pressure significantly drop across that fluid barrier. This behavior has been observed in comparable fields in the USA as well. The overall shape of fluid flow direction trends in a SW–NE direction. Main recharge occurs by infiltration of surface water into the faults, especially in the southwest and near to Lake Linau. Discharge is enhanced in highly fractured areas toward Lake Linau. Vertical permeability of faults allows fluids rising toward the hot springs at surface.

Results show that permeability has to be considered for simulation of a geothermal system. The geothermal system is mainly controlled by fluid flow in fractures/faults depending on temperature and pressure conditions. The locally modified fluid flow can considerably influence the productivity of a geothermal field. Results also guide reservoir management in case of a potential for field extension, as performed in Lahendong.

References

Brehme M, Regenspurg S, Zimmermann G (2011) Hydraulic-hydrochemical modelling of a geothermal reservoir in Indonesia. Mineral Mag 75:577

Brehme M, Haase C, Regenspurg S, Moeck I, Deon F, Wiegand BA, Kamah Y, Zimmermann G, Sauter M (2013) Hydrochemical patterns in a structurally controlled geothermal system. Miner Mag 77:767. doi:10.1180/minmag.2013.077.5.2

Brehme M, Moeck I, Kamah Y, Zimmermann G, Sauter M (2014) A hydrotectonic model of a geothermal reservoir—a study in Lahendong, Indonesia. Geothermics 51:228–239. doi:10.1016/j.geothermics.2014.01.010

Brehme M, Deon F, Haase C, Wiegand B, Kamah Y, Sauter M, Regenspurg S (2016) Geochemical properties controlled by fault permeability in a geothermal reservoir (Lahendong, Indonesia). Grundwasser 21:29–41. doi:10.1007/s00767–015–0313–9

Cherubini Y, Cacace M, Blöcher G, Scheck-Wenderoth M (2013) Impact of single inclined faults on the fluid flow and heat transport: results from 3-D finite element simulations. Environ Earth Sci 70:3603–3618. doi:10.1007/s12665-012-2212-z

Delisle G, Beiersdorf H, Neben S, Steinmann D (1998) The geothermal field of the North Sulawesi accretionary wedge and a model on BSR migration in unstable depositional environments. Geol Soc Lond Spec Publ 137:267–274. doi:10.1144/GSL.SP.1998.137.01.21

DHI-Wasy (2009) FEFLOW white papers, vol 1, 368 pp

Diersch H-JG (2014) Finite Element modeling of flow, mass and heat transport in porous and fractured media. Springer, Berlin, p 996

DWD, Deutscher Wetterdienst (2007) Offenbach/Main. http://www.dwd.de/. Accessed June 2012

Haneberg WC (1995) Steady state groundwater flow across idealized faults. Water Resour Res 31:1815–1820

Hooper ECD (1991) Fluid migration along growth faults in compacting sediments. J Pet Geol 14:161–180. doi:10.1111/j.1747-5457.1991.tb00360.x

Hölting B, Coldewey W (2005) Hydrogeologie: Einführung in die allgemeine und angewandte Hydrogeologie. Springer, Berlin

Johnson-Maynard J, Anderson M, Green S, Graham R (1994) Physical and hydraulic properties of weathered granitic rock in southern California. Soil Sci 158:375–380

Kaya E, O'Sullivan MJ, Hochstein MP (2014) A three dimensional numerical model of the Waiotapu, Waikite and Reporoa geothermal areas, New Zealand. J Volcanol Geotherm Res 283:127–142. doi:10.1016/j.jvolgeores.2014.07.008

Klavetter E, Peters R (1987) An evaluation of the use of mercury porosimetry in calculating hydrologic properties of tuffs from Yucca Mountain, Nevada, Nevada Nuclear Waste Storage Investigations Project Report. Project-Report, Nevada Nuclear Waste Storage Investigations Project

Koestono H, Siahaan EE, Silaban M, Franzson H (2010) Geothermal model of the Lahendong geothermal field, Indonesia. In: Proceedings World Geothermal Congress 2010, Bali, Indonesia, 25–29 April 2010

Magri F, Akar T, Gemici U, Pekdeger A (2011) Numerical investigations of fault-induced seawater circulation in the

Seferihisar–Balçova geothermal system, western Turkey. Hydrogeol J 20:103–118. doi:10.1007/s10040-011-0797-z

McGuinness M, White S, Young R, Ishizaki H, Ikeuchi K, Yoshida Y (1995) A model of the Kakkonda geothermal reservoir. Geothermics 24:1–48. doi:10.1016/0375-6505(94)00020-D

Mercer JW, Faust CR (1979) Geothermal reservoir simulation: 3. Application of liquid-and vapor-dominated hydrothermal modeling techniques to Wairakei, New Zealand. Water Resour Res 15:653–671. doi:10.1029/WR015i003p00653

Milsch H, Priegnitz M, Blöcher G (2011) Permeability of gypsum samples dehydrated in air. Geophys Res Lett 38:6. doi:10.1029/2011GL048797

Moeck IS (2014) Catalog of geothermal play types based on geologic controls. Renew Sustain Energy Rev 37:867–882. doi:10.1016/j.rser.2014.05.032

Nagao T, Uyeda S (1995) Heat-flow distribution in Southeast Asia with consideration of volcanic heat. Tectonophysics 251:153–159

Neben S, Hinz K, Beiersdorf H (1998) Reflection characteristics, depth and geographical distribution of bottom simulating reflectors within the accretionary wedge of Sulawesi. Geol Soc Lond Spec Publ 137:255–265. doi:10.1144/GSL.SP.1998.137.01.20

O'Sullivan MJ, Pruess K, Lippmann MJ (2001) State of the art of geothermal reservoir simulation. Geothermics 30:395–429. doi:10.1016/S0375-6505(01)00005-0

Ondrak R, Wenderoth F, Scheck M, Bayer U (1998) Integrated geothermal modeling on different scales in the Northeast German basin. Geol Rundschau 87:32–42. doi:10.1007/s005310050187

Popov Y, Pribnow D, Sass J (1999) Characterization of rock thermal conductivity by high-resolution optical scanning. Geothermics 28:253–276

Schön JH (2004) Physical properties of rocks. Elsevier Ltd, Amsterdam

Saghravani S, Yusoff I, Mustapha S, Saghravani S (2013) Estimating groundwater recharge using empirical method: a case study in the tropical zone. Sains Malays 42:553–560

Sutherland R, Toy VG, Townend J, Cox SC, Eccles JD, Faulkner DR, Prior DJ, Norris RJ, Mariani E, Boulton C, Carpenter BM, Menzies CD, Little TA, Hasting M, De Pascale GP, Langridge RM, Scott HR, Reid Lindroos Z, Fleming B, Kopf J (2012) Drilling reveals fluid control on architecture and rupture of the Alpine fault, New Zealand. Geology 40:1143–1146. doi:10.1130/G33614.1

Wiegand BA, Brehme M, Teuku F, Amran IA, Prasetio R, Kamah Y, Sauter M (2013) Geochemical and isotopic investigation of fluids from Lahendong geothermal field. Miner Mag 77:2491. doi:10.1180/minmag.2013.077.5.23

Yani A (2006) Numerical modelling of the Lahendong geothermal system, Indonesia, Report from United Nations University